

Severe Accident Sequence Analysis

Part 1: Analysis of Postulated Core Meltdown Accident Initiated by Small Break LOCA in Kori-1 PWR Dry Containment

Jong In Lee, Seung Hyuk Lee and Jin Soo Kim

Korea Advanced Energy Research Institute

Byung Hun Lee

Han Yang University

(Received June 13, 1984)

고리 1호기 소형파단 냉각제 상실사고에 의해 개시된
가상 노심용융 사고 해석

이 증 인 · 이 승 혁 · 김 진 수

한국에너지연구소

이 병 현

한양대학교

(1984. 6. 13 접수)

Abstract

An analysis is presented of key phenomena and scenario which imply some general trends for beyond design-basis-accident in Kori-1 PWR dry containment. The study covers a wide range of severe accident sequences initiated by small break LOCA. The MARCH computer code, with KAERI modifications was used in this analysis. The major emphasis of the paper are two folds, 1) the phenomenologic understanding of severe accident and 2) a study of H₂ combustion and debris/water interactions in a specific small break LOCA for Kori-1 plant. The sensitivity studies for the specific plant data and thermal interaction modelings used in the SASA were performed. The results show that if hydrogen burning does occur at low concentration, the resulting peak pressure does not exceed the design value, while the lower concentration assumption results in repeated burning due to the continuing H₂ generation. For debris/water interaction, the particle size has no effect on the magnitude of peak pressure for the amount of water assumed to be in the reactor cavity. But, the occurrence of peak pressure is considerably delayed in case of using the dryout correlation. The peak containment pressure predicted from the hydrogen combustion and steam pressure spike during full core meltdown scenario does not present a severe threat to the containment integrity.

요 약

고리 1호기의 소형파단냉각제 상실사고에 의해 개시된 중대사고 유형과 그 현상에 대한 분석이 제

시되었다. 본 해석에서는 KAERI에서 기존 전산코드의 수정·보완된 MARCH 전산코드가 사용되었다. 특히 코리 1호기의 소형파단 LOCA 해석시 수소 거동과 증기과압에 대한 평가 및 그 응답성에 중점을 두고 검토되었으며, 2-loop 발전소 데이터 분석 및 debris-water 상호작용 모델에 대한 비교 분석이 수행되었다. 제 1부 중대 사고유형 분석결과, 저농도에서 H₂ burning이 이루어지는 경우 계속적인 수소 생성으로 인해 반복 수소 spike가 야기되나, 격납용기 설계압력치 보다 낮게 예측되었다. 또한 debris/water 상호작용시 core debris의 입자크기는 침투압력의 크기에 미치는 영향은 미세하나 침투압력의 발생시점은 dryout 모델사용에 의해서 상당히 지연시키게 되었다. 완전한노심용융 사고시 수소연소와 증기과 압으로부터 예측된 격납용기 최대압력은 격납용기 건전성에 심각한 위협을 초래하지 않는 것으로 나타났다.

1. Introduction

The accident at TMI-2 has shown the usefulness of the probabilistic risk assessment (PRA) methodology, since the Reactor Safety Study (RSS)¹⁾ had already noticed the possibility of such accident and predicted the accident sequences quite well. Thereafter, there has been a growing need for the application of PRA techniques in certain areas of reactor safety assessment. In fact, several PRA studies^{2),3)} on individual nuclear power plants have been completed or are in progress in the United States, and NRC has prepared a comprehensive procedures guide⁴⁾ to complement the present licensing methodology by using this technique. There is no doubt that PRA technique would play an important role in the field of reactor safety evaluation and in new safety issues in the future. However, uncertainties exist in many areas of the analysis and the details of the phenomena at the various phases of severe accident are not understood well at present.

Of particular interest in this work is the development of the capability to simulate a wide range of postulated transients and accident conditions for beyond design-basis accidents, in order to gain insights into the measures that can be taken to improve reactor safety. The cooling of degraded core, and fully molten core initiated by transients and small break LOCA in PWR is of special importance. This is necessary

for investigating failure conditions in order to improve aspects of plant design and operation of engineered safety features (ESF) which may require regulatory attention.

In an effort to keep up with the trends in foreign countries and to assess the importance of new safety issues for the future, severe accident sequence analysis (SASA), which is one of the essential parts of PRA, was performed for the Kori-1 plant. In the analyzed accident, the hypothetical core meltdown accident was initiated by small break LOCA with and without ECCS. In this study, modified MARCH code⁵⁾, with KAERI modifications, was utilized. Among the modifications were the considerations of the various in-vessel and ex-vessel debris/water interactions, the extended modeling of metal-water reaction, time step control, and the computational procedures and logic.

The objectives of this study are two folds as follows,

- (1) an assessment of applicability of current core meltdown scenarios in developing the severe accident mitigation measures for the future, and
- (2) Investigation of the potential hydrogen burning and steam pressure spike for Kori-1 plant.

For the above purposes, an extensive sensitivity study was performed to verify the effects of specific plant design and parameters on the accident behavior, and also specific effects, such as the various break size, hydrogen flammability limits in the containment, and in-vessel and

ex-vessel debris/water interaction are investigated. In addition, primary emphasis was laid on the phenomenological understanding of core meltdown sequences and the pressure-temperature responses of containment building.

2. Accident Description

2.1. Initiating Event

Small and large break LOCA and any kind of transients analyzed deterministically in safety analysis report could result in core meltdown accident, i.e, severe accident, when combined with the failure of a certain ESF system.

The general trend is to select small break LOCA or transients as the initiating event. In this paper, small break LOCA with and without ECCS was analyzed by using the modified March computer code for the Kori-1 nuclear power plant. Accumulators and containment heat removal system, which consists of spray system and fan cooler system, were assumed to have actuated as designed. Analyses of transient cases will be carried out later and results will be presented separately as a link in the chain of severe accident sequence analysis.

2.2. March Code Description

The principal core meltdown computer model developed for use in RSS was the Boil code,⁶⁾ originated by BCL, and improvements and extensions to Boil were undertaken subsequent to RSS to generalize its application to accident sequences other than the large LOCA, to enhance consistency, and to incorporate new experimental data. The current version is entitled March (Meltdown Accident Response Characteristics) in which the Boil code is incorporated as an essential subroutine, and it provides a continuous, coupled analysis of the thermal and hydraulic response of the LWR systems to small or large pipe break and transient accidents

which could result in core meltdown when combined with the failure of ESF. This code performs the calculation from the time of the commencement of the accident through the stages of blowdown, core heatup, boiloff, core meltdown, pressure vessel bottom head melting and failure, debris-water interaction in the reactor cavity and the interaction of the molten debris with the concrete containment base pad. The mass and energy additions into the containment with or without ESF are calculated. The March code was modified by safety analysis group at KAERI. The major changes in phenomenological modeling are the treatment of core debris/water interaction with and without gas upflow, the improved metal-water reaction, and the computational procedures and logic.

The containment can be divided into segments of upto 8 interconnected compartment volumes and the ESFs that can be modeled include the ECCS, CSS, CFCS, and recirculation heat exchangers. This code could carry out the calculations through the 6 stages of accident sequences as follows.

(1) Heatup of the primary and secondary coolant inventories and pressure rise due to the relief/safety valve settings with the subsequent boiloff,

(2) Initial blowdown of the primary system coolant into the containment, and generation and transport of heat within the core and associated coolant,

(3) Heatup of the fuel following core uncover, including the effects of zircaloy-water reactions, melting and slumping of the fuel onto the lower core support structure and into the vessel bottom head,

(4) Interaction of the core debris with water and gas upflow in the reactor cavity following melt-through of the vessel,

(5) The molten debris/concrete interaction due to attack of the concrete basement, and

(6) Effects on the containment pressure and temperature responses of the steam pressure spike, burning of hydrogen, and other combustibles.

2.3 General Assumptions and Computational Methods

1) Containment model

Kori-1 containment is a complex of two separate structures with 5-foot annular space between walls. The inside containment vessel is a cylindrical steel pressure vessel with hemispherical dome and torispherical bottom and is completely enclosed by a reinforced concrete shield building having a vertical cylindrical shape with a spherical segment roof. To simplify the calculation and due to some restrictions of March code, a simple model of the containment structure was assumed in which the annular gap between walls was not considered. Four heat slabs and two different materials are modelled to simulate the containment, internal miscellaneous steels, and concrete base pad.

Containment response predictions are essential for most accident analyses the radiological consequences increase markedly if the containment fails due to the static overpressurization or the hydrogen burns. As March uses a simple empirical natural convection wall heat transfer model, the large error would occur when forced convection transients are induced by rapid steam generation (e, g, blowdown, molten debris-coolant contact) or rapid noncondensable gas generation (e, g, hydrogen generation or combustion). Thus, March predicts the containment pressure too conservatively (over-prediction) and needs improvement on the wall heat transfer model. However, very little information exists for forced and natural convective condensation heat transfer model with large noncondensable gas fractions.

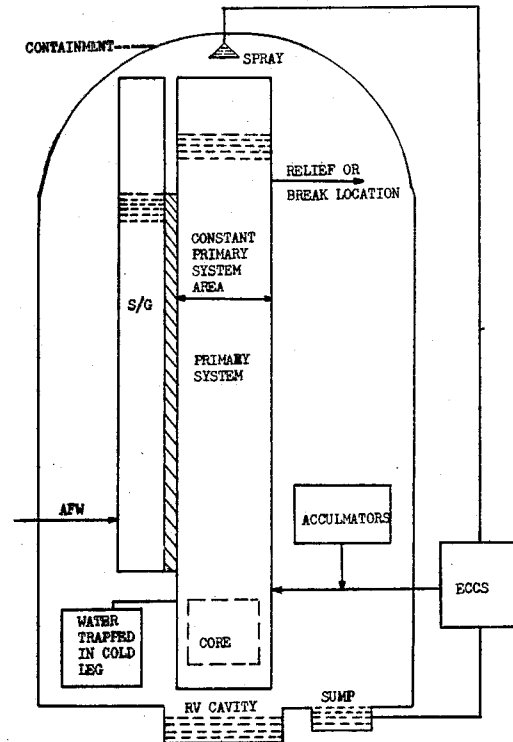


Fig. 1. MARCH Nodalization of the Volume of the Primary and Secondary Coolant Systems for Kori-1 Plant

2) Primary system model

Fig. 1 shows the nodalization of primary system volumes. March code models the primary system as one cylindrical volume with liquid at the bottom and gases at the top. A small sub-compartment (containing liquid in thermodynamic equilibrium with the liquid in the large volume) is used to simulate water trapped in the cold legs during boiloff and added to containment when head fails. This code assumes that all coolant injected into the primary system immediately mixes and thermally equilibrates with the existing in-vessel liquid. There is no evaporation of liquid injected above the in-vessel water level, either through a hot leg, or from a core spray system.

3) Core heatup and boiloff model

Energy is generated during this of the accident by decay heat and by exothermic metal-

water oxidation reactions. The fission-product decay heat formulation in ANS 5.1⁷⁾ is used to calculate the source term for decay heating. The oxidation reaction rate of zirconium at the surface may be inhibited by either gas phase diffusion or by the formation of a protective barrier film through which the reactor vapor and gaseous reaction products must diffuse.

March assumes that the reaction rate is limited by the minimum of these two rate mechanisms. The gas-phase diffusion limit uses a Nusselt number approach as originally formulated by Baker and Just⁸⁾ and a choice between two parabolic reaction-kinetics models can be used (Baker-Just or Cathcart)⁹⁾ to model the solid-state diffusion. In this study, Baker-Just model is utilized.

The core heat transfer models account for (1) convective heat transfer between the fuel rods and steam or water coolant, (2) radiation heat transfer from the fuel rods to steam and from the uncovered nodes to structures above the core or to water below the nodes (3) heat transfer resulting from the quenching of the slumped molten core material and recovered nodes.

4) Meltdown model

There are 3 core meltdown models (model A, B, C) in March which are not phenomenological in the sense that slumping is not based on calculations of stress levels, creep rates, or flow rates of molten materials. Fuel slumping is triggered when a fuel node reaches the melting point of the core and absorbs additional energy equal to the latent heat of fusion. In meltdown model A, the excess heat in the molten pool is assumed to propagate downward. This model maximizes the downward movement of the molten pool. In model B, it is assumed that that excess heat in the molten pool is transferred upward, and in model C, it is assumed that when a fuel node melts, it immediately

falls to the bottom of the pressure vessel. Thus, model A is physically consistent with a melt-down situation in which the molten region tends to cover and mix (downward) with the solid region at such a rate the homogenized molten region remains just at the melting temperature. Hence model A is used in the present work.

5) Debris/water interaction for in-vessel and ex-vessel analysis

The thermal interactions of the hot core debris/water and molten core debris with concrete are of particular importance for the investigation of debris bed coolability. In a light water reactor, the interaction of the core debris with water first occurs in the bottom head of the reactor vessel, which could result in the complete evaporation of the reactor vessel water, and then, the failure of the reactor vessel. After that, the hot core materials initially make contacts with the water in the ex-vessel and/or the water discharged directly from the emergency core cooling system.

The previous analysis of the debris/water interaction with the March⁵⁾ code was based on the single sphere model. This model implies that on the order of at least million spheres will fall into the reactor cavity, but it is uncertain that all of the particles would establish close contacts with water. As such, the assumption that total surface area is available for heat transfer may not be valid. The actual debris/water interaction is much much more complicated than that described by single sphere model. As an alternative approach, the porous debris bed models applied by Yang¹⁰⁾ can be used to analyze the potential in-vessel and ex-vessel debris/water interaction. The porous bed is assumed to be formed by spherical debris particles. The porosity, permeability and the average particle size control the dynamics of the vapor and liquid flow in the porous system. The

Table 1. Kori-1 Plant Data

Design Parameters	Used Value
1. Containment Building	
Free volume, ft ³	1.45 × 10 ⁶
Design pressure, psia	58
Initial pressure, psia	14.7
Initial Temperature, °F	120
2. Primary System and Core	
Water volume, ft ³	6579
Steam Volume, ft ³	400
Mass U ₂ O ₃ in Core, lb	1.22 × 10 ⁵
Mass Steel in Core, lb	2.44 × 10 ⁴
Mass Zr in Core, lb	2.443 × 10 ⁴
Mass bottom head, lb	7.65 × 10 ⁴
Bottom head diameter, ft	11
Bottom head thickness, ft	0.344
Initial core power, Btu/hr	5.898 × 10 ⁹
Initial system pressure, psia	2250
Initial avg. coolant temp, F°	577
Initial S/G secondary water mass, lb	1.556 × 10 ⁵
Flow of core area, ft ²	27
Core diameter, ft	8.04
Fuel rod diameter, ft	0.03517
Clad thickness, ft	0.002023
3. Accumulator Tank	
Total mass of water, lb	1.22 × 10 ⁵
Actuation pressure, psia	700
Water temperature, F	120
4. Containment Spray System	
Actuation pressure, psia	38
Spray flow rate, gpm	3200
Spray water temp., F	120
5. Containment Fan Cooler	
Cooling capacity (4 fans), Btu/hr	2 × 10 ⁸
Air flow rate, cfm	1.46 × 10 ⁵
Secondary flow rate, lb/min	2.85 × 10 ⁵
Primary inlet temp, F	213
Secondary inlet temp., F	95

debris cooling and steam generation are controlled by the hydrodynamics of the two-phase flow and also the porous models developed by many researchers were examined and applied to test their impact on containment dynamics by Yang¹⁰⁾, square¹¹⁾, and Lee¹²⁾. In this work, the dryout model developed by Lipinski¹³⁾ for the assessment of steam pressure

spike (e.g. overpressurization) was used, and the comparison analysis between dryout correlation and single sphere model is presented in the results.

2.4 Plant Information

Data for the Kori-1 nuclear power plant are provided for the classes of accident considered in this paper. The design parameters¹⁴⁾ for the plant is given in Table 1. In the cases where input data generation was not possible, some reference plant data¹⁵⁾ were utilized.

3. Results and Discussion

An analysis of small break LOCA with and without containment ESF as a part of severe accident sequence analysis is studied for Kori-1 PWR dry containment plant. It is assumed that the reactor cavity contains 2.778 × 10⁵ lbs of water prior to vessel failure. This is the maximum amount of water that could be available in the cavity at this time, as predicted by the modified MARCH code. About 1.22 × 10⁵ lbs. of water is from the accumulators and 2.58 × 10⁵ lbs. is obtained by redirecting all of the water that otherwise would have gone into the sump. The selection of accident sequence studies (such as S₁B, S₂B, S₁D and S₂D) is based, in part, on WASH1400.¹⁾ In this study, no attempt is made to determine the probability of the accidents or a dominant accident sequence.

Several parametric studies were performed for the analysis of the above sequences. The effects of break size were studied for S₁B and S₂D sequences by varying the equivalent break diameter from 2 inches to 3 and 5 inches. Uncertainties in the hydrogen burn characteristics were studied by assuming a range of flammability limits from 10–0% to 8–4% for S₂D sequence. In ex-vessel analysis, the impact of the uncertainty of the heat transfer rate is

demonstrated for the different model of debris-water interaction.

3.1 Small (S₂) LOCA with Containment ESF

1) Reference Case

For the base case, the bulk of the data presented assumes an equivalent break diameter of 2 inches. Two variations of small LOCA with heat removal system-maximum and minimum safeguards-were considered for the heat removal effects. 2 spray pumps and 4 containment building cooling fans for the maximum cases were assumed to be operating, which for minimum safeguards 1 pump and 2 fans were assumed to be operating from the time of the accident. The containment building spray pumps were assumed to operate only after containment building pressure of 38 psia had been reached. In the base case, the single sphere model was used to estimate the debris/water heat transfer rate.

In both cases, the progression of the Zr-H₂O reaction and core melting is shown in Figure 2. An observable Zr-H₂O reaction precedes initial core melting by approximately 300S. The

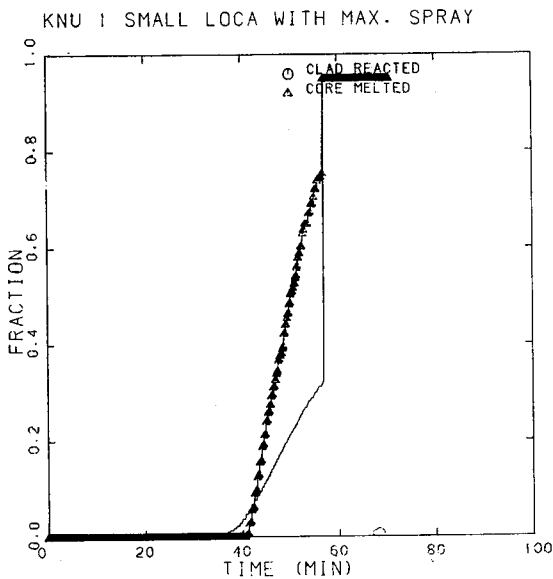


Fig. 2. Fraction of Clad Reacted and Core Melted During S₂D Sequence

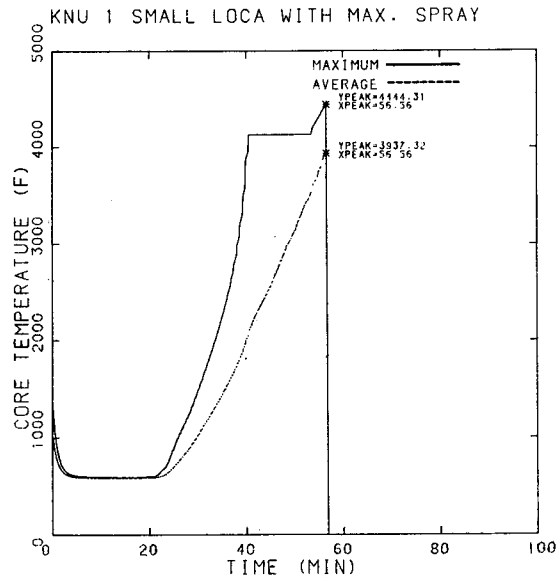


Fig. 3. Core Temperature Profiles as a Function of Time for S₂D Accident

model specifies that the core will slump into the lower plenum when the fuel temperature at the center of the core, as shown in Figure 3, approaches the UO₂ boiling temperature. At this point, the code predicted that approximately 75 % of the core is melted and 32% of the Zr is reacted (Figure 2). All the remaining Zr was reacted with water in the reactor cavity following failure of the bottom head. MARCH predi-

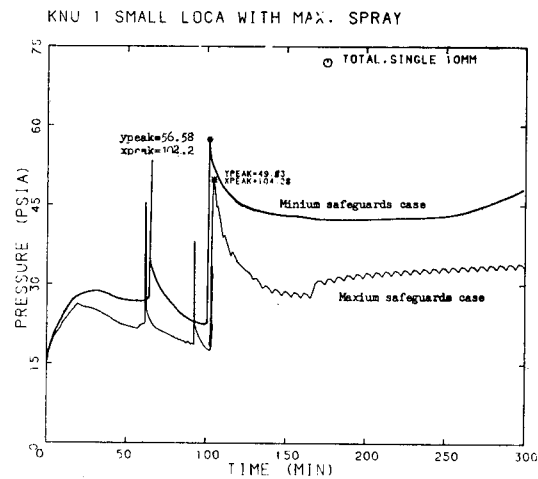


Fig. 4. Containment Transient Pressure for the S₂D Maximum and Minimum Safeguards (Single Sphere Model)

Table 2. Results for Large Dry Containment Kori-1 Plant S₂D Sequence

Initiating Event	S ₂ D Maximum Safeguards		S ₂ D Minimum Safeguards		S ₂ B Sequence	
	Accident Time(min.)	Containment Pressure(pisa)	Accident Time(min.)	Containment Pressure(psia)	Accident Time(min.)	Containment Pressure(psia)
Cooler on	0.0	14.7	0.0	14.7	—	—
Core uncover	20.78	26	22.23	28.13	21.17	31.0
Start melt	40.9	23.5	42.37	27.91	141.5	46.43
Core slump	50.8	21.68	57.8	26.32	168.3	45.8
1st H ₂ burn	61.45	48.0	66.27	56.1	—	—
Spray on	61.96	—	66.78	—	—	—
End of boil	70.33	21.43	71.54	28.64	187.5	52.16
2nd H ₂ burn	92.3	40.8	—	—	—	—
Head fail	102.9	18.09	101.4	22.27	230.3	51.51
Debris quenched	104	49.63	102	56.58	—	—
Recirculation on	165	27.5	171.7	42.49	—	—

cted very rapid rates for Zr-water reaction and evaporation of water when molten materials slump into either the lower head or the reactor cavity. These rates resulted in a primary pressure spike when the core slumps into the lower plenum. Representative graph of the transient containment pressure is shown in Figure 4. Figure 4 illustrates the effect of heat removal for the S₂D sequences. The first spike is the result of the burning of hydrogen in both maximum and minimum cases. Both variations follow similar trends except that the minimum safeguards variation produced slightly higher steam pressure in the containment building. The results, from the detailed data of Table 2, indicate that core slumping occurs rather earlier for the S₂D cases (51 minutes for maximum case and 58 minutes for minimum case) than for the S₂B sequence (168 minutes). This is presumably due to the lower containment pressure in the S₂D cases allowing faster blowdown and removal of the primary system water. The main issue from both S₂D sequences is that operation of the cooling fans reduces the steam pressure in the containment building below the pressure obtained in the case where the containment building safeguards were not used. However, the removal of steam from the cont-

ainment building by the cooler again increases the potential of H₂ ignition and burning, which is discussed below.

2) Sensitivity studies on H₂ Burning

Various kinds of parameter concerning H₂ burning effect on the thermal-hydraulic behavior of the containment. Several sensitivity studies are performed to look at the quantitative effects of the parameters, such as flammability limit, burning time and spray effect, on peak pressure and temperature. Majority of hydrogen burns considered in this work are based on the MARCH burning model. The hydrogen ignition point and lower limit must be specified by user and they both are based on the volume fraction of hydrogen in containment atmosphere. The only constraint on hydrogen burning is that oxygen concentration must exceed 6.5% volume fraction. For the burning model, there is experimental evidence to indicate that combustion may be incomplete for lean hydrogen concentrations. The experimental results by Slifer¹⁶⁾ showed very incomplete combustion of hydrogen up to 8% initial hydrogen volume fraction and almost complete consumption for hydrogen volume fraction over 6%. Another experimental studies¹⁷⁾ have been performed on burning concentration and time, but the information is not

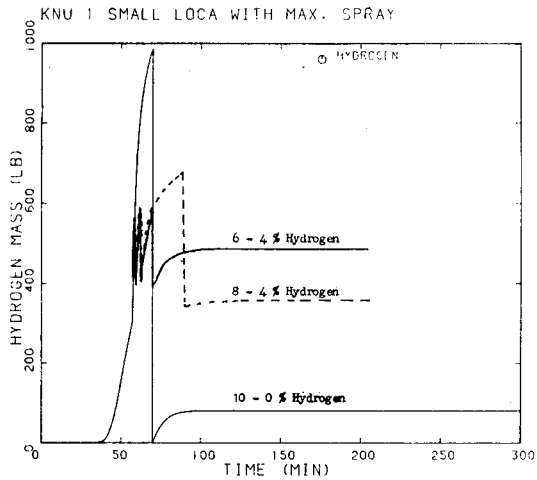


Fig. 5. H₂ Production and Consumption for S₂D Accident

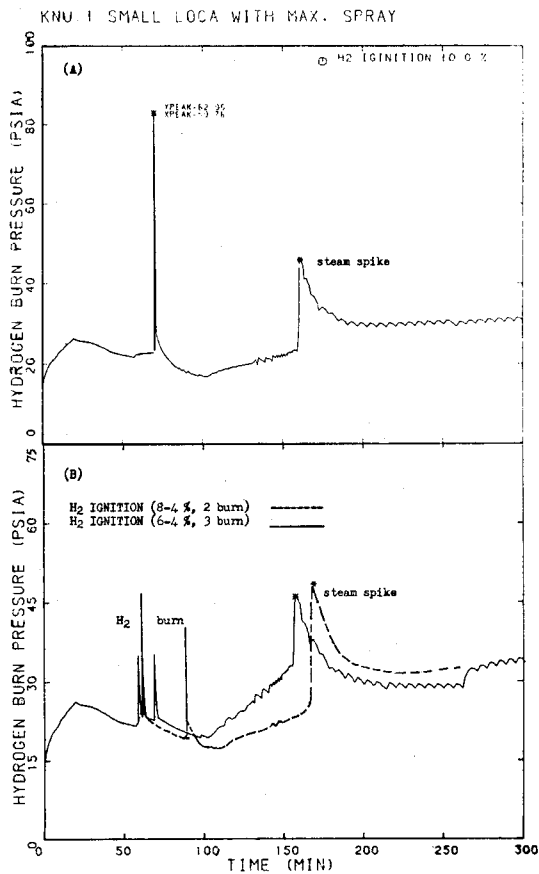


Fig. 6. Comparison of Adiabatic Hydrogen Burn Pressure for Different Flammability Limit

sufficient for the application to the large volume case such as the containment. Based on those experimental results, we have considered the possibility of three combustion scenarios of 6-4%, 8-4% and 10-0% hydrogen volume fraction.

The effects of assuming the alternative hydrogen combustion scenarios in S₂D maximum safeguard sequence are shown in Figures 5 and 6. Figure 5 indicates that the hydrogen produced by metal-water reaction is about 1200 lbs. for in-vessel calculation. The hydrogen burns, which occur at the point of flame limit as shown in Figure 6 depend on the ignition point. The effects of hydrogen burns for concentrations from 8% down to 4% in Figure 6 (b) are not significantly different from the cases of 6-4% concentration for S₂D sequences. Only the hydrogen burns are slightly later because it takes longer to reach the higher concentration. The pressure trends from the burns are of the same order of magnitude for both cases. In Figure 6 (a), the upper flammability limit is assumed to be 10% and the lower limit 0%. Under these circumstances only one burn occurs in the compartment with large pressure rises (83 psia) due to the combustion of a large quantity of hydrogen. It is significant that the frequency of burns drops but their magnitude increases, compared to the other cases (46 psia for 8-4% and 34 psia for 6-4% case). However, we noted above that hydrogen may not burn to completion at the lean flammability limit. Table 3 gave the peak values of pressure and temperature for the different burning initiating concentrations and burning times. From those results, it is understood that the longer burning time and lower initiating concentration show the lower peak pressures. But it must be considered that the effect of burning time is dependent on the heat transfer coefficient to the structural heat sinks and that the lower

Table 3. Peak Pressure and Temperature at H₂ Burning

Case No.	burning Concentration (%)	burning time (sec)	spray flow (gpm)	occurrence time (min.)	H ₂ consumed (lb)	peak pressure (psia)	peak temperature (F)
1	10-0	6.6	3,200	70.39	989	83.1	1,934
2	10-0	0.6	1,600	95.78	1,067	89.4	1,744
3	8-4	0.6	3,200	61.18	392	47.9	895
4	8-4	3.0	3,200	61.51	393	48.0	987
5	804	0.6	1,600	66.01	457	56.1	900
6	6-4	6.0	No	61.64	199	35.9	536

initiating concentration assumption results in repeated burnings due to the continuing H₂ generation. If a severely degraded core is not avoided, our preliminary assessment indicates that some sequence will prevent steam overpressurization for dry cavity case¹²⁾ but that could aggravate the problem of hydrogen ignition and burning. Recently, various hydrogen control concepts have been proposed to protect the containment against the hydrogen burning and detonation. Among these concepts are a filtered vent system, water fog system, oxygen depletion system and containment pre-inerting system. If these systems could be used effectively, the pressure rise would be caused by the debris/water interaction alone. It is seen that, without H₂ burning, the pressure rise is well below the estimated containment failure pressure.

3) Steam Pressure Spike

For certain postulated core meltdown accidents, large quantities of hot core debris may contact with water in the containment cavity after vessel failure. Those debris/water interaction may yield rapid generation of steam, which in turn causes rapid pressurization of the containment building. It is very important to accurately analyze the steam generation rates associated with debris/water interactions. In the original MARCH code, a single sphere model is used to estimate the debris/water heat transfer rates in which case the internal and surface heat transfer are the dominant controlling mechanisms. Hence, the model implies that the

interaction of debris/water is not water limiting and the total surface area of all spheres is available for heat transfer from hot debris particles to the water. Since millions of debris particles could be formed when the core falls into the cavity, it is uncertain that all particles would be in close contact with water. An alternative model¹³⁾ applied by Yang¹⁰⁾ was used in this study for evaluating the improved debris/water interaction. This model assumes that the core debris forms a porous debris bed and that the heat removal is controlled by the dryout heat flux characteristics of the debris bed. Some model with upflow gas and its application have been presented in the previous paper¹⁸⁾.

The effect of different modelings for core debris/water interaction on the containment pressure transient is illustrated in Figure 4 for single sphere model and Figure 7 for dryout correlation model. The use of debris bed correlation for evaluating steam production in the reactor cavity has eliminated the rapid steam spikes predicted by single sphere model, but the eventual containment pressure is predicted to be higher, largely due to the effect of steel water reactions. As shown in Figure 7, the effect of particle size is assessed as the part of the debris/water interaction. For the 50mm particle size, the large heat transfer from the debris to water yields a very rapid quenching of the particles and releases a large amount of sensible heat. An instant pressure spike is generated in the containment building, could caused by the

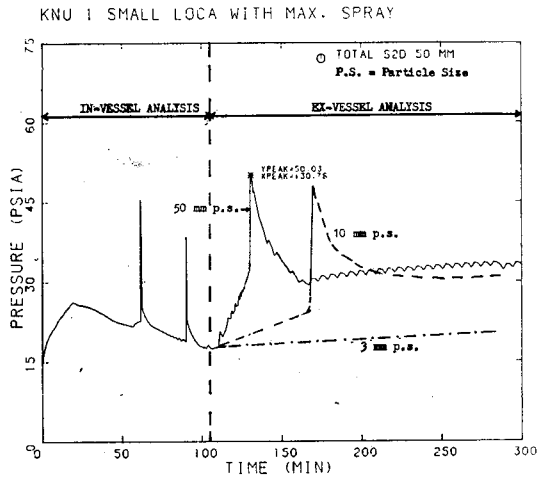


Fig. 7. Effect of Particle Size on Containment Pressure for Using Debris Bed Model

rapid evaporation of the cavity water. For the smaller particles (3mm), the rise of the pressure spike is slightly slower as the heat transfer is relatively smaller. On the other hand, the predicted peak pressure from the 3mm single model is higher than that of the larger spheres, since small sphere increases the total surface

and, hence, the total heat transfer rate. After the core debris quenching, the decay heat is the major source for steam generation and pressure buildup. The particle size size no longer plays an important role in the containment dynamics and has no effect on the magnitude of peak pressure for the amount of water assumed to be in the reactor cavity. But the quenching time, at which the first peak pressure occurs, strongly depends on the particle size as shown in Figure 7. The small particles make water penetration more difficult and thus delay the quenching time and the occurrence of the first peak pressure in the ex-vessel analysis.

3.2 Small(S₁) LOCA with Failure of ESF Power

1) Basic Case

we assessed the influence of break area on small LOCA (S₁B, S₂B) accident progression. A representative graph is shown in Figure 8. Figure 8 indicates the containment transient pressure histories for a range of break areas in

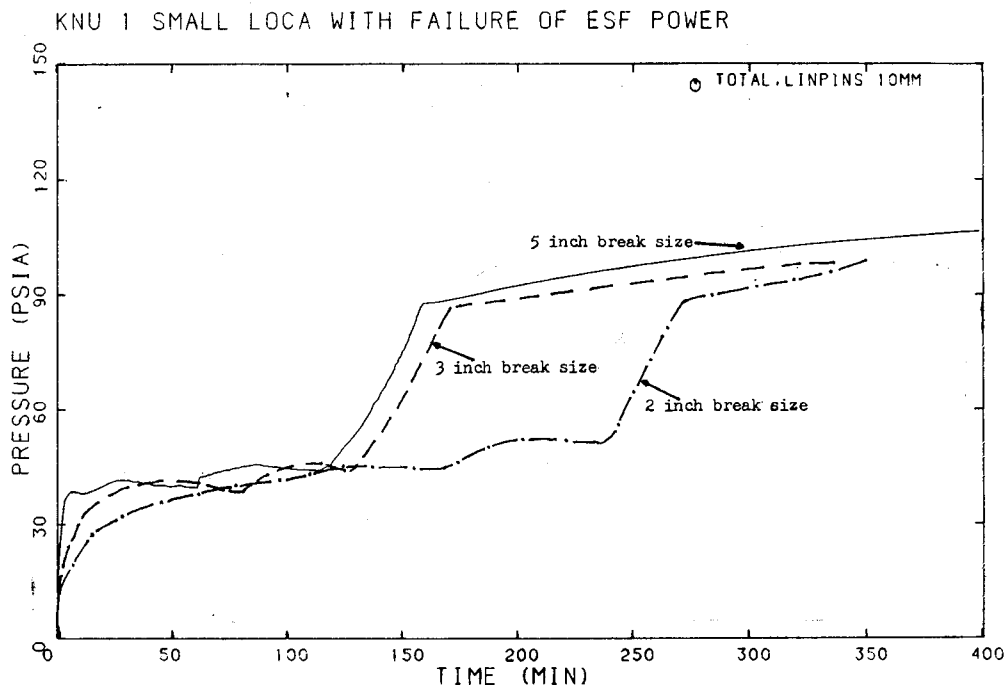


Fig. 8. Effect of Break Size on Containment During S₁B Sequence (Flooded Cavity Case)

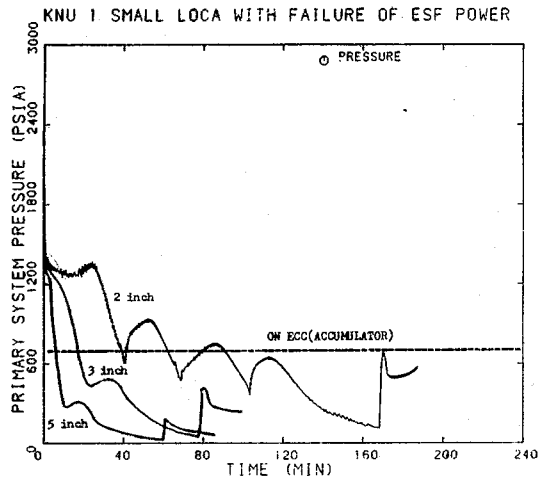


Fig. 9. Primary System Pressure Trends as a Function of Time for S_1B Sequence

Kori-1 plant. The results show that core slumping occurs at 60 minutes for the 5 inches break area as compared with 168 minutes case. Head failure is predicted to take about one hour for both cases with resulting head failure times of 107 and 230 minutes for the 5 and 2 inch cases, respectively. Accumulator injection, which depends on the primary system pressure, occurs much earlier for the large break area as shown in Figure 9. In Figure 9, the accumulators inject water intermittently until the core slumping, and the continuous injection of the accumulators is prevented by the repressurization of the primary system, but for the larger break this phenomena is not observed by MARCH run. The effect of large break area is to accelerate depressurization of the primary system, and the consequent earlier core slumping and head failure time appear to result in higher containment pressure. This impact would appear reasonable as slower steam flow rates into the containment building would allow more time for condensation and heat transfer to the walls resulting in lower steam pressure. The different pressure trends for the S_1B sequence, compared with S_2B case, are due to the injection of accumulator

water. The water reaches its boiling temperature after head failure, and a steady evaporation rate is maintained by heat removal according to the dryout heat flux model. Hence the containment pressure shows a steady increase until all debris particles are quenched. After that, the steam generation is mainly caused by the decay heat, which yields a slower pressure rise.

2) Water Inventory in Ex-vessel

We examined the effect of a substantial quantity of water in Kori-1 reactor cavity. The effect of flooded cavity relative to Kori-1 small break LOCA with failure of ESF power is shown in Figure 10. The impact of having water in the reactor cavity prior to head failure for the large break case is rather more dramatic than for small break case. For the smaller break area, water remains in the accumulator at head failure even if the cavity is assumed to be initially dry, there is an interaction of the core debris with accumulator in the reactor cavity. However, for the larger break case all the accumulator is injected into the reactor vessel before head failure so that if the cavity is assumed to be dry, there is obviously no ex-vessel interaction of core debris with accumulator water. MARCH predicts that the effect of injecting all the accumulator water into the vessel for the S_1B sequence results in the earlier core slumping and head failure, and consequently in higher containment pressure as shown in Figure 8.

The amount of water in the cavity was assumed to be sufficiently large so that the interaction with core debris is not water limited. If the coolable core debris geometry was assumed, the core debris temperature of about 3,800 F at the point of head failure is cooled to 360F and then the pressure reaches 88 psia at the time of debris quenching in the containment building. After the debris quenching, the core debris is brought into thermal equilibrium with water and all the sensible energy in the core

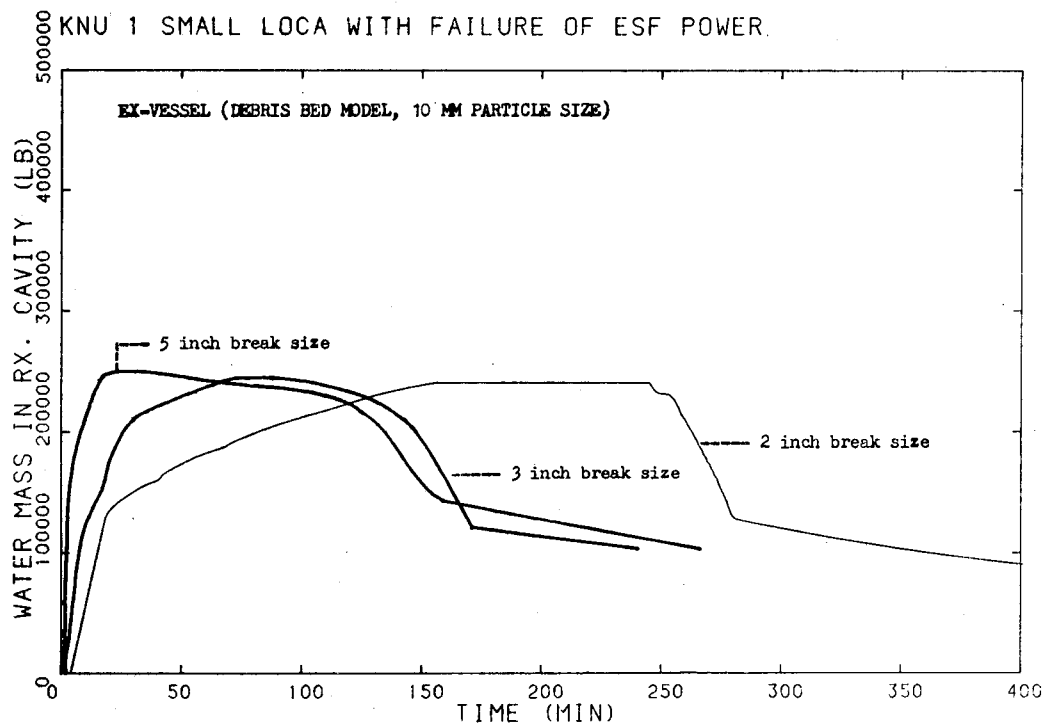


Fig. 10. Variation of Water Mass in Reactor Cavity (Flooded Cavity Case)

debris goes to vaporizing water. The continuous boiling of water by decay heat continues to gradually pressurize the containment atmosphere due to overcome condensation. It is clear from the above results that MARCH predicts significantly greater pressurization for the flooded cavity case than for the dry cavity case⁽¹²⁾.

4. Summary and Conclusions

The following conclusions can be made from the results of this study.

(1) Containment thermal-hydraulic analysis computer code (MARCH) was modified to treat the improved thermal interactions under severe accident.

(2) Containment thermal-hydraulic behavior during the hypothetical core meltdown accident (initiated by small break LOCA) of 600 MWe Kori-1 PWR with reinforced containment vessel was studied.

(3) For the S₂D sequence, sensitivity studies on H₂ burning were performed. The predicted maximum adiabatic pressure during H₂ burning at low concentration does not threaten the containment integrity. The effect of burning time is dependent on the heat transfer coefficient to the structural heat sinks and the lower concentration assumption results in repeated burning due to the continuing H₂ generation.

(4) Comparison studies on the modelings of debris/water interaction were carried out. The use of debris bed correlation for evaluating steam production in the reactor cavity has eliminated the rapid steam spike predicted by the single sphere model, but the eventual containment pressure is predicted to be higher. The particle size no longer plays an important role in the containment dynamics and has no effect on the magnitude of peak pressure for the amount of water assumed to be in the reactor cavity.

(5) For S₁B sequence, the effect of large break area is to accelerate depressurization of the primary system, and results in the earlier core slumping and head failure time, which in turn appear to cause higher containment pressure.

(6) For full core meltdown accident, containment integrity and core debris coolability could be achieved if an effective H₂ control system and long term containment cooling system can be maintained.

(7) The additional emphasis of this paper not only determines the thermal hydraulic conditions in such accidents, but also provides the interested researchers with the information on the important phenomena, especially H₂ burning and steam pressure spike, which must be studied in detail from the point of the PWR safety.

References

1. Reactor Safety Study, An Assessment of Accident Risks in the U.S. Commercial NPPs, WASH-1400 (1975)
2. U.S. NRC, preliminary Assessment of Core melt Accidents at the Zion and Indian NPPs and Strategies for Mitigating their Effects, NUREG-0850, Vol. 1 (1981)
3. Gregory J. Kolb, et al., Interim Reliability Evaluation Program; Analysis of the Arkansas-1 NPP, SAND 82-0978, Vol. 1 (1982)
4. U.S. NRC, PRA Procedures Guide, NUREG/CR-2300, (1983)
5. R.O. Wooton and H.I. Avci, MARCH Code description and User' Manual, NUREG/CR-1711, BMI-2064, BCL (October 1980)
6. R.O. Wooton, Boil 1, a Computer Program to Calculate Core Heatup and Meltdown in a Coolant Boiloff Accident, BCL (March 1975)
7. Proposed ANS standard decay energy Release Rates following shutdown of Uranium-Fueled Thermal Reactors, ANS 5-1 (Oct. 1971)
8. L. Baker and L.C. Just, Studies of Metal-water Reactions at High Temperatures III Experimental and Theoretical Studies of the Zirconium-water Reaction, ANL, ANL-6548 (May 1962)
9. J.V. Cathcart, Quarterly Progress Report on the Zirconium Metal-water Oxidation Kinetics Program, ORNL, ORNL/NUREG/TM-87 (Feb. 1977)
10. J.W. Yang and W.T. Pratt, Steam Pressure Spike in PWR Plant under Severe Accident Conditions, Int. Mtg. on Thermal Reactor Nuclear Safety, Chicago (August 1982)
11. D. Squarer and A.T. Pieczynski, Effect of Debris Bed Pressure, Particle Distribution on Degraded Nuclear Reactor Core Coolability, Nuclear Reactor Core Coolability, Nucl. Science and Eng. 80, 2-13 (1982)
12. J.I. Lee, An Evaluation on Containment Transient Pressure Under Postulated Core Meltdown Accident, Informal Report, BNL (to be published)
13. R.J. Lipinski, A Particle Bed Dryout Model with Upward and downward Boiling, ANS. Trans. Vol. 35, p. 358 (1980)
14. Final Safety Analysis Report for Kori NPP unit No. 1, Korea Electric Company (1976)
15. Indian Point Probabilistic Safety, Edison Company (1982)
16. B.C. Slifer and T.G. Peterson, Hydrogen Flammability and Burning Characteristics in BWR Containments, NEDO-10812, General Electric (April 1973)
17. M. Hertzberg, Flammability Limits and Pressure Development in H₂-Air Mixtures, NUREG/CR-2017 (Sep. 1981)
18. Jong In Lee and Jin Soo Kim, An evaluation of Cooling of Core debris and impact on Containment Transient Pressure under Severe Accident Conditions, J. of KNS Vol. 15, No. 4 (Dec. 1983)